

Robotic reconstitution of cytostatic drugs and monoclonal antibodies: transforming aseptic drug compounding in hospital pharmacies

Geersing, T.H.

Citation

Geersing, T. H. (2025, March 19). Robotic reconstitution of cytostatic drugs and monoclonal antibodies: transforming aseptic drug compounding in hospital pharmacies. Retrieved from https://hdl.handle.net/1887/4198886

Version: Publisher's Version

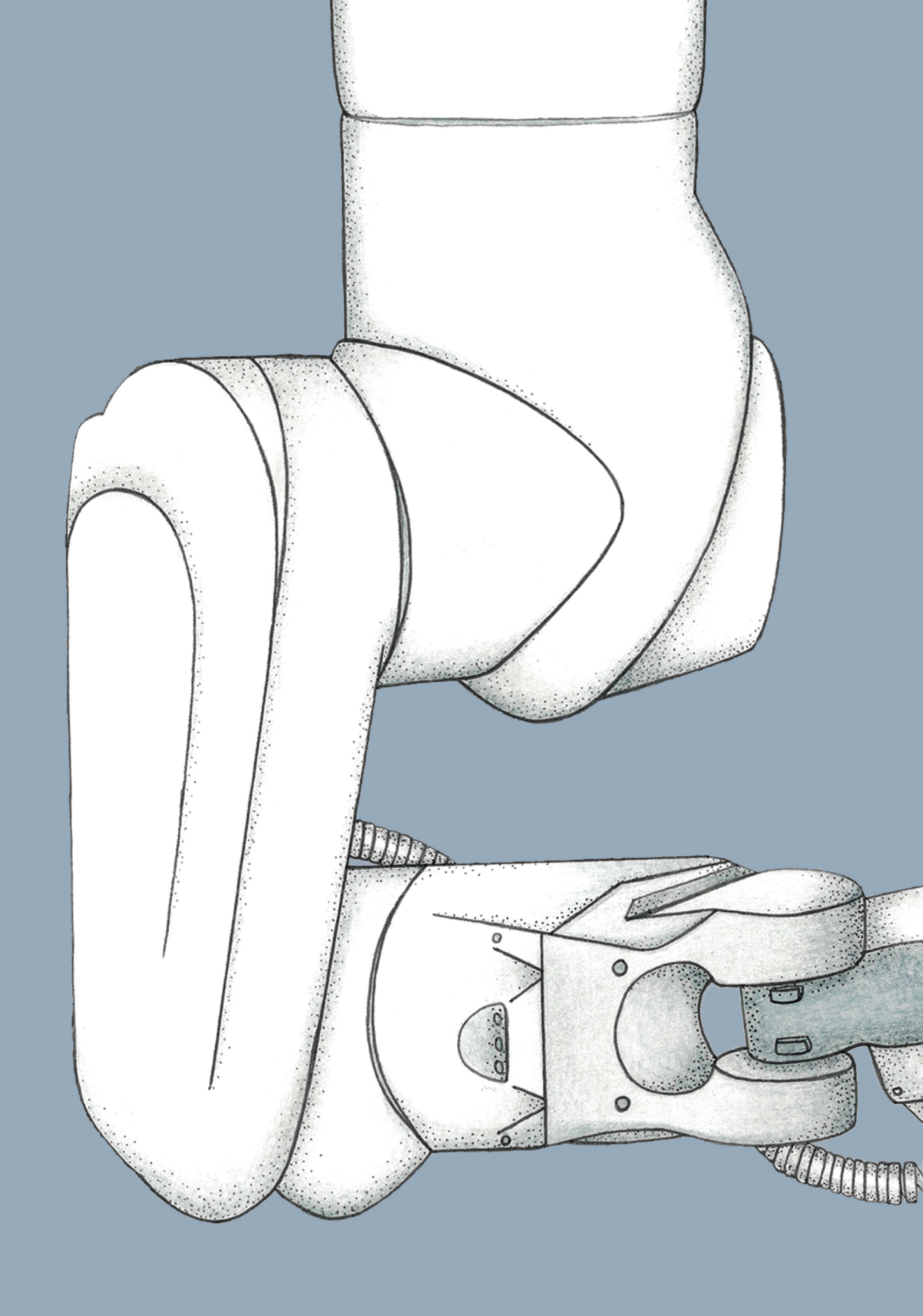
Licence agreement concerning inclusion of doctoral

License: thesis in the Institutional Repository of the University

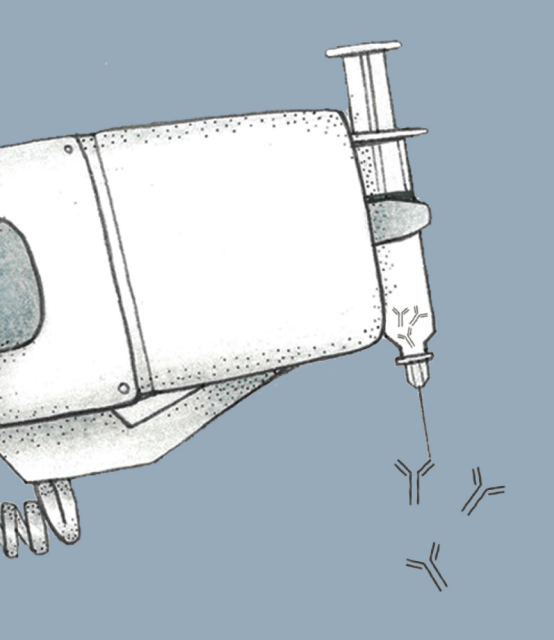
of Leiden

Downloaded from: https://hdl.handle.net/1887/4198886

Note: To cite this publication please use the final published version (if applicable).



Aggregate formation and antibody stability in infusion bags: the impact of manual and robotic compounding of monoclonal antibodies



Tjerk H. Geersing, Dunja Dogan, M. Reza Nejadnik, Stefan Romeijn, Catherijne A.J. Knibbe, Mirjam Crul

ABSTRACT

Monoclonal antibodies (mAbs) can be damaged during the aseptic compounding process, with aggregation being the most prevalent form of degradation. Protein aggregates represent one of several risk factors for undesired immunogenicity of mAbs, which can potentially lead to severe adverse drug reactions and less effective treatments. Since data on aggregate and particle formation by robotic compounding is missing, we aimed to compare the antibody stability between robotic- and manual compounding of mAbs with regard to formation of (sub)visible aggregates. Infliximab and trastuzumab were compounded into infusion bags with the APOTECAchemo robot or manually by nurses or pharmacy technicians. The products were analyzed by quantifying (sub)visible particles with nanoparticle tracking analysis, dynamic light scattering (DLS), light obscuration, micro-flow imaging, high pressure size exclusion chromatography (HP-SEC), and visual inspection. HP-SEC showed high percentages monomers in trastuzumab (99.4% and 99.4%) and infliximab (99.5% and 99.6%) infusion bags for both manual and robotic compounding, respectively. DLS indicated more consistent and reproducible results with robotic compounding, and confirmed monodisperse samples with a higher polydispersity index for manual compounding (0.16, interquartile range; IQR 0.14-0.18) compared to robotic compounding (0.12, IQR 0.11-0.15). This study shows that the studied compounding methods had a minor impact on the number of aggregates and particles, and that robotic compounding of mAbs provided at least similar quality as manual compounding.

INTRODUCTION

The compounding of drugs is a high-risk area of pharmacy practice for both patients and healthcare workers. Risks that can seriously impact patient safety include errors in product identification, drug compounding and dilution, final product labeling, and issues with sterility and dose accuracy. The evolution of robotic compounding has mitigated some of these risks for patients and healthcare workers and has had broad impact on society. Firstly, it improves patient waiting times and satisfaction. Furthermore, it minimizes the risk of human error and lowers the risk of pain or injury due to repetitive hand movements. It also reduces the risk of exposure to hazardous drugs for pharmacy technicians, which does not apply for monoclonal antibodies (mAbs) as these are not classified as hazardous drugs. Another problem that could be solved by the use of robots for compounding is the scarcity of pharmacy technicians. Only one person is needed to operate a compounding robot compared to the two-to-three pharmacy technicians needed for conventional manual compounding. Last but not least, robotic systems also have a positive social impact by reducing costs and drug waste.

In 2021, the Amsterdam University Medical Centre (Amsterdam UMC) purchased the fully automatic APOTECAchemo robot. Our research group previously investigated the robot's microbiological performance, environmental and external cross-contamination, dosing accuracy and precision, time consummation, and performed an economic evaluation of vial sharing of expensive drugs. 8-12 Currently, the robot in Amsterdam UMC is being used for the aseptic compounding of 13,000 cytostatic drug preparations (70%) per year. The scarcity of pharmacy technicians in the Amsterdam area and the fast growth of treatments with biopharmaceuticals, especially mAbs, has led to consideration of the usage of the robot for compounding mAbs.

mAbs are, however, complex and delicate molecules and protein pharmaceutical products are advised to be handled with care. Jiskoot et al. listed several potential issues with the conventional compounding of biologicals in a hospital that might jeopardize product quality. These include, among others, vigorous manual agitation of the vials, formation of air bubbles in the syringes, formation of foam in the vials, repetitive upand-down movement of plungers of syringes containing protein formulations, ignorance of the occurrence of turbidity in protein formulations in the syringes, and nonuniform homogenization procedures for intravenous infusion bags. Such protein-destabilizing conditions should be avoided to keep purity levels high and prevent formation of aggregates and other impurities.

The compounding process of mAbs has been shown to exert numerous stresses that can potentially result in protein aggregation. Moreover, exposure to foreign materials can contribute to the particle load by shedding nonproteinaceous microparticulate and nanoparticulate materials into the solution. Hearmacy technicians and nurses handling the mAb play a significant role in ensuring the quality and prevention of degradation of the protein products. Swirling the vial gently without shaking it and slowly drawing it into the syringe is especially critical. The APOTECchemo robot shows more abrupt movements during compounding, potentially leading to additional stress on the product. Protein aggregates are one of the several risk factors that can lead to undesired immunogenicity, adverse drug reactions (ADRs) and to a less effective treatment. Therefore, it is important to ensure that compounding does not compromise the safety and efficacy of the therapeutic products.

Studies that investigate the use of robots for compounding of mAbs are scarce. One study, addressed compounding of three mAbs (bevacizumab, infliximab, and trastuzumab) with the i.v.STATION® robotic arm. Aggregation was measured using five different analytical methods: UV-Vis absorbance, 90° light scatter, intrinsic fluorescence emission, Nile Red fluorescence microscopy, and field flow fractionation without focus and cross flow. The analytical methods showed that reconstitution according to the summary of product characteristics does not lead to detectable aggregation in both robotic and manual compounding. ¹⁵ Up until now, there is no published research about the stability of mAbs compounded with the APOTECAchemo robot. This study aims to compare the quality between robotic- and manual compounding of mAbs concerning antibody stability and formation of (sub)visible aggregates. The quality will be assessed using six analytical techniques: nanoparticle tracking analysis (NTA), dynamic light scattering (DLS), light obscuration (LO), micro-flow imaging (MFI), high-performance size exclusion chromatography (HP-SEC), and visual inspection.

MATERIALS AND METHODS

Monoclonal Antibodies

The following mAbs were used: Herzuma 150 mg powder for concentrate for solution for infusion (trastuzumab, batch numbers 18A4C23C2 and 18A4C25C1, Celltrion Healthcare, Hungary) and Remsima 100 mg powder for concentrate for solution for infusion (infliximab, batch numbers 0B3N496 and 0B3N571, Celltrion Healthcare, Hungary).

Compounding of infusion bags

Trastuzumab 150mg and infliximab 100mg were compounded into 250ml sodium chloride 0.9% infusion bags (Viaflo infusion bags, Baxter, Illinois, USA, batch numbers 21G01E3K / 21H07E3Y / 21I24E3S / 21J21E3E / 21K15E3U / 21K27E3T) resulting in concentrations of 0.54 mg/ml and 0.36 mg/ml, respectively. These preparations were performed to obtain concentrations similar to those at the lower end of the therapeutic range. Negative controls were performed out of 0.9% sodium chloride infusion bags after each sample in MFI, LO and visual inspection. In total 44 infusion bags were compounded, among which four were used as positive controls (one manually and one robotic compounded bag per drug). From the remaining 40 infusion bags, 18 infusion bags were manually compounded by pharmacy technicians and nurses in the Amsterdam UMC, location VUMc (fig. 1). The other 22 infusion bags were compounded using the APOTECAchemo robot (Loccioni, Italy). Robotic compounding comprised the full compounding process from drug powder in a vial to protein solution in a bag. Siliconized syringes with preassembled needles (AEA srl, Angeli di Rosora, Italy) were needed during robotic compounding, while spikes (Codan, Lensahn, Germany) were used with manual compounding. Water for injection (Fresenius Kabi, Germany, batch number 19QGB160) was used to dissolve the mAbs. For each trastuzumab infusion bag, a sideline (Codan Connect Z[®], Codan BV, the Netherlands) was used to resemble real-world compounding as much as possible. The infusion bags containing infliximab were prepared using an inline, sterile, non-pyrogenic, low protein-binding 0.2 µm filter (Codan I.V.STAR®).

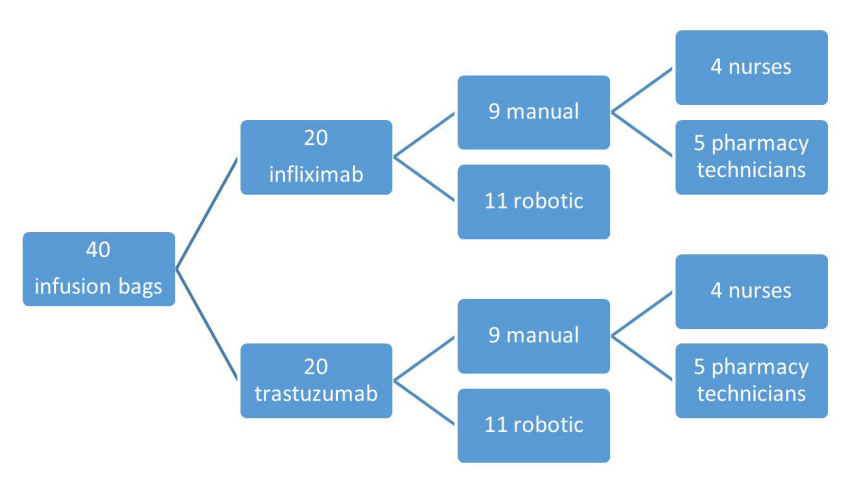


Fig. 1. Schematic overview of infusion bags produced with robotic and manual compounding.

Stressing monoclonal antibodies (positive controls)

Antibody products serving as positive controls were exposed to a combination of stresses, simulating possible compounding errors induced by manual or robotic compounding. Two types of stress were used to create aggregates, aspiration/dispense (AD) cycles and shaking, such that a significant increase in sub-visible particles was obtained while monomer loss as a percentage was kept minimal. The infusion bags were aspirated and dispensed 15 times through an 18G (1,2 mm x 40 mm) needle (BD Microlance, New Jersey, USA). Thereafter, the bags were exposed to shake stress, by attaching them to the IKA Vibrax VXR Basic (IKA-Werke, Germany) and shaking it with orbital agitation at 1000 rpm and a shaking stroke of 4 mm for 16 hours at room temperature. The infusion bags were placed horizontally onto the shaker to increase the movement of the fluid inside ¹⁷

Product Characterization

After the compounding of mAbs in infusion bags in Amsterdam UMC, the bags were transported to the Leiden Academic Centre for Drug Research for analysis. The influence of this transport was analysed in a preliminary study, in which trastuzumab and infliximab were manually compounded in Amsterdam and Leiden by the same technician. All analyses were conducted usually within two days but no later than within four days after compounding. Samples were collected in tubes on the day of analysis by puncturing through the medication port with a 18G (1.2 mm x 40 mm) needle (BD Microlance, New Jersey, USA). Both infusion bags and samples were stored at room temperature. The formation of aggregates and particles was determined by analyzing each product with high-performance size exclusion chromatography (HP-SEC), nanoparticle tracking analysis (NTA), dynamic light scattering (DLS), light obscuration (LO), micro-flow imaging (MFI), and visual inspection.

High Pressure Size Exclusion Chromatography

HP-SEC was used to detect and quantify the amount of protein monomer, dimer, and aggregates in the products. The analysis was performed using a Yarra 3u SEC-2000 300 \times 7.8mm column (Phenomenex, California, USA) on an Agilent 1200 chromatography system (Agilent Technologies, California, USA) including an Agilent UV detector at a flow rate of 0.5 mL/min. One hundred μl of each product was injected. The mobile phase was composed of 50 mM sodium phosphate dibasic dihydrate, 150 mM L-Arginine monohydrochloride, and 0.025% sodium azide (Sigma-Aldrich, Missouri, USA) at pH 6.5. To quantify monomers and other species, UV absorption at 280 nm was recorded with ChemStation Software (Agilent Technologies).

Nanoparticle Tracking Analysis

NTA was used to determine the concentration of particles between 30 nm and 1000 nm. Measurements were performed with a NanoSight LM20 (NanoSight, Amesbury, UK) equipped with a sample chamber with a 640-nm laser. All measurements were performed at room temperature, and all products were injected undiluted. The product samples were injected into the chamber by an automatic syringe pump (Harvard Apparatus, catalog no. 98–4362, Holliston, USA) using a sterile 1 mL syringe (BD Discardit II, New Jersey, USA). For each product, a 60-second video was captured using the "single shutter and gain mode", with the shutter set at 1500 and the gain at 680. Three measurements of the same sample were performed for all infusion bags. Videos were captured and analyzed using the NTA 2.0 Build 127 software. The following settings were used for tracking the particles: background extract on, brightness 0, gain 1.00, blur size 3 × 3, detection threshold 10, and viscosity equal to that of water. All other parameters were set to the automatic adjustment mode.

Dynamic Light Scattering

Dynamic Light Scattering (DLS) was used to detect particles in the nanometer size range in accordance with the research of Filipe et al. DLS is a robust method that provides information about the average size of the particles in the formulation and their polydispersity. DLS measurements were performed with a Malvern Zetasizer Nano ZS (Malvern Panalytical, United Kingdom) equipped with a 633 nm He-Ne laser and backscattering was measured at an angle of 173 degrees. One mL of the product samples was analyzed in disposable polystyrene macro cuvettes (Brand®, The Netherlands) with a path length of 10 mm. The measurements were executed at a position of 4.65 mm from the cuvette wall with an automatic attenuator and a controlled temperature of 25 degrees Celsius. For each sample, 10 runs of 15 seconds were performed, with three repetitions. The intensity size distribution, the Z-average diameter (Z-ave), and the polydispersity index (PdI) were calculated from the correlation function using the Dispersion Technology Software version 7.03 from Malvern. All product samples were measured undiluted.

Light Obscuration

The particle size (size range 1 μ m - 200 μ m) and corresponding concentration were established with Light Obscuration (LO). Measurements were performed on a PAMAS SVSS system (PAMAS Partikelmess- und Analysesysteme GmbH, Germany) equipped with an HCB-LD-25/25 sensor and a 1-mL syringe. ¹⁸ Each sample was measured three times, with each measurement consisting of a pre-run volume of 0.3 mL followed by three runs of 0.2 mL at a flow rate of 10 mL/min.

Micro-Flow Imaging

The size, concentration, and morphology of particles in the infusion bags were established with micro-flow imaging (MFI). MFI can detect micron-sized particles up to 100 μ m. An MFI5200 system (ProteinSimple, Santa Clara, USA), equipped with a silane-coated flow cell (1.41 × 1.76 × 0.1 mm) and controlled by the MFI View System Software version 2, was used for flow imaging microscopy analysis. The system was flushed with 6 mL of purified water at 6 mL/min before each measurement, and the flow cell cleanliness was checked visually between measurements. The background was zeroed by flowing NaCl 0.9% through the system and performing the "optimize illumination" procedure. Then, 0.9 mL of each product sample was analyzed at a flow rate of 0.17 mL/min, with a purge volume of 0.2 mL and a fixed camera shot rate of 22 flashes per second. The data recorded by the system software was analyzed with MFI View Analysis Suite version 1.2.

For each product, stuck, edge, and slow-moving particles were removed by the software before data analysis. The equivalent circular diameter (ECD) was calculated and presented as a measure of the particle size $(1-100 \mu m)$.

Visual inspection

Visual inspection was performed by gently inverting, swirling, and observing the samples in standard room illumination for a minimum of five seconds against both a white and black background. The presence of any visible particles was recorded.

Data Management and Statistical Analysis

All data were recorded in Excel 16 (Microsoft Office, Redmond, USA) on protected servers in the IT environment at LACDR and St. Antonius hospital. No personal information from the pharmacy technicians and nurses was recorded or stored. In order to compare the differences between manual and robotic compounding, the nonparametric Mann-Whitney U test was performed using IBM SPSS Statistics 25 (Statistical Package for the Social Sciences, Illinois, USA).

RESULTS

All infusion bags were analyzed using six complementary techniques covering a size range from particles of 10 nm in diameter up to visible particles. The results are summarized in Table 1, which also includes the differences in monomers, dimers, and, oligomers between manual- and robotic compounded bags analyzed with HP-SEC. Submicron particles of the same bags were analyzed with NTA and DLS (fig. 2), and micron particles were analyzed with LO (fig. 3) and MFI (fig. 4). A preliminary analysis of

four bags, compounded in Amsterdam and Leiden, has shown that transport from Amsterdam to Leiden did not play a major role in the formation of (sub)visible aggregates (supplementary information, table 1).

Table 1. Overview of results of the product characterization experiments in manually and robotic compounded infusion bags.

Technique	Detection range	Inflix	cimab	Trastuzumab			
		Manual (n=9)	Robotic (n=11)	Manual (n=9)	Robotic (n=11)		
HP-SEC	Amount monomer (%)	99.4	99.4	99.5	99.6		
	Amount dimer (%)	0.6	0.6	0.3	0.3		
	Amount oligomers (%)	0.0	0.0	0.2	0.0		
NTA	Size range: <1 μm	N/A ^a	N/A ^a	N/Aª	N/A ^a		
DLS	Size range: <1 μm	+	-	0	0		
LO	Size range: ≥1 μm	+	-	0	0		
MFI	Size range: ≥1 μm	+	-	0	0		
VI	Size range: ≥100 μm	present	present	present	present		

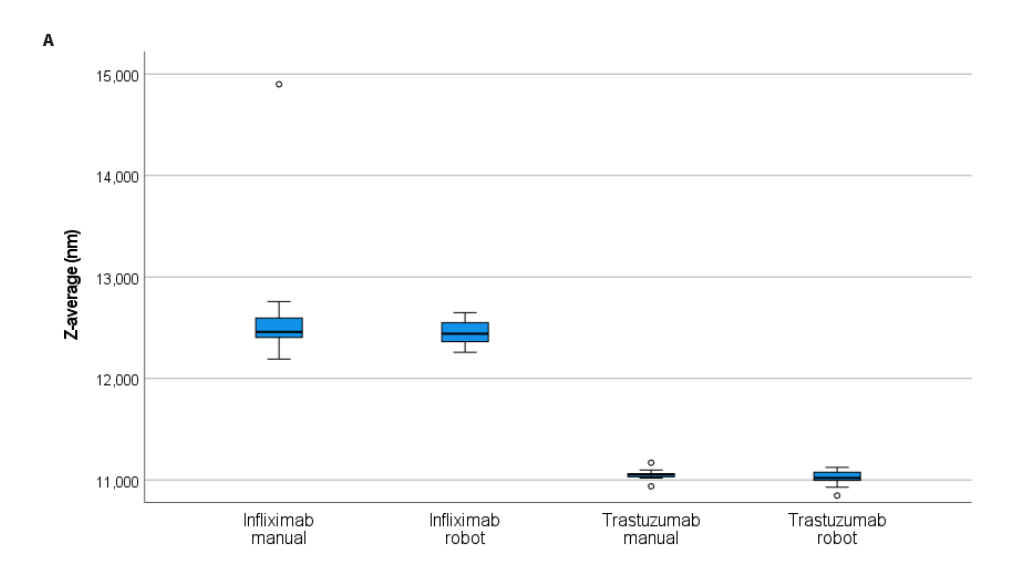
⁺ Significant higher number of particles in manual compounded bags versus robotic compounded bags

The HP-SEC analysis of manual and robotic compounded bags showed that all infusion bags had a minimum of 99.4% monomer content (table 1). There was 0.6% dimer in the infliximab bags and 0.3% dimer in the trastuzumab bags. Oligomers other than dimers were only found in the manually compounded trastuzumab infusion bags. In addition, HP-SEC chromatograms showed similar results for manual and robotic compounded bags in both infliximab and trastuzumab samples (supplementary information, fig. 2 and 3).

⁻ Significant lower number of particles in robotic compounded bags versus manual compounded bags

⁰ No significant difference between manual and robotic compounded bags

^a number of particles was below the limit for quantitative analysis



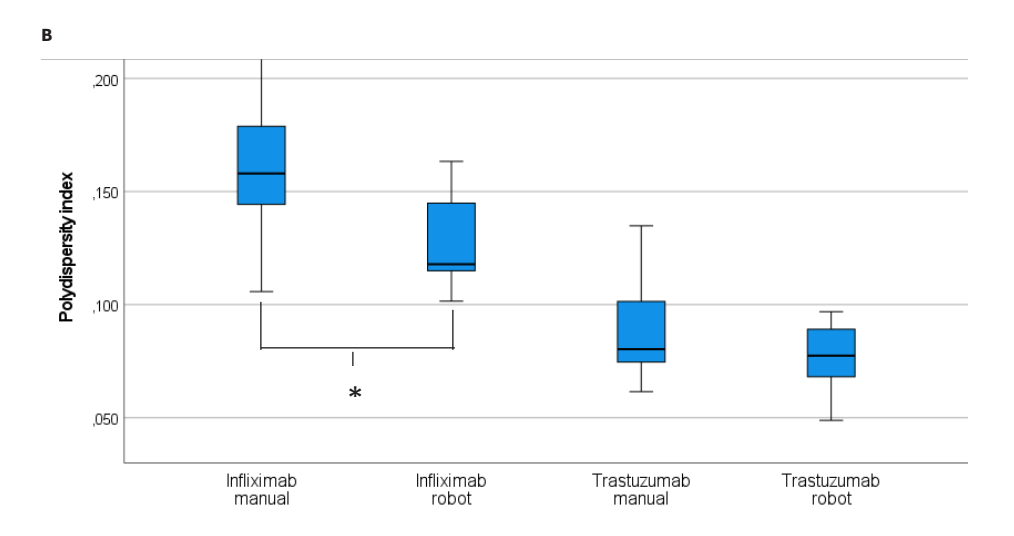
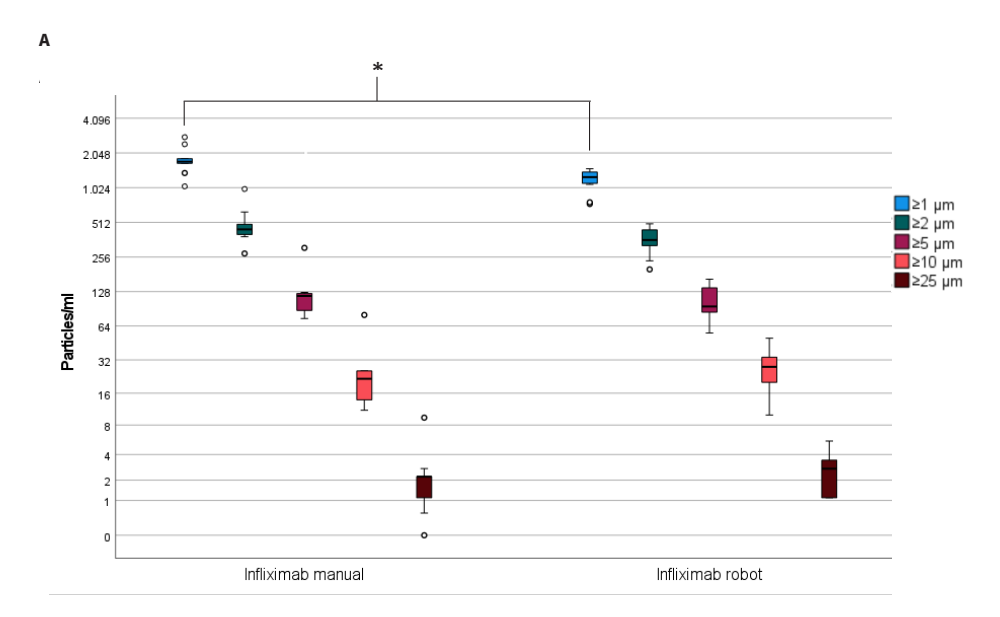


Fig. 2. Dynamic light scattering results in infliximab and trastuzumab infusion bags after manual- and robotic compounding. The boxplots show the median, interquartile range and the 5%/95% range with T-bars. A) Monomer size. Outliers are represented with open dots. B) The polydispersity index. The nonparametric Mann-Whitney U test was used for statistical analysis (*p < 0.05).



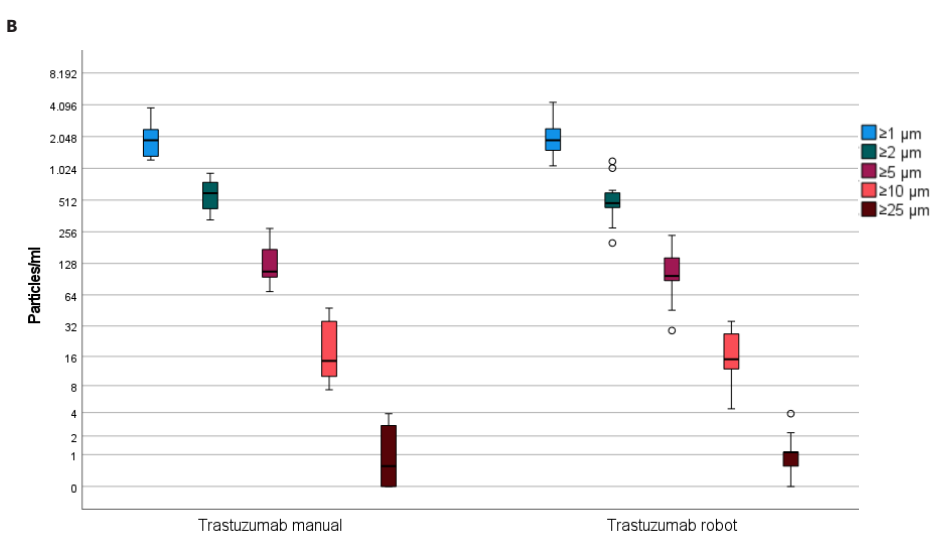


Fig. 3. Light obscuration results (concentration of particles) in infliximab A) and trastuzumab B) infusion bags after manual and robotic compounding. The boxplots show the median, interquartile range and the 5%/95% range with T-bars. Outliers are represented with open dots. The nonparametric Mann-Whitney U test was used for statistical analysis (*p < 0.05).

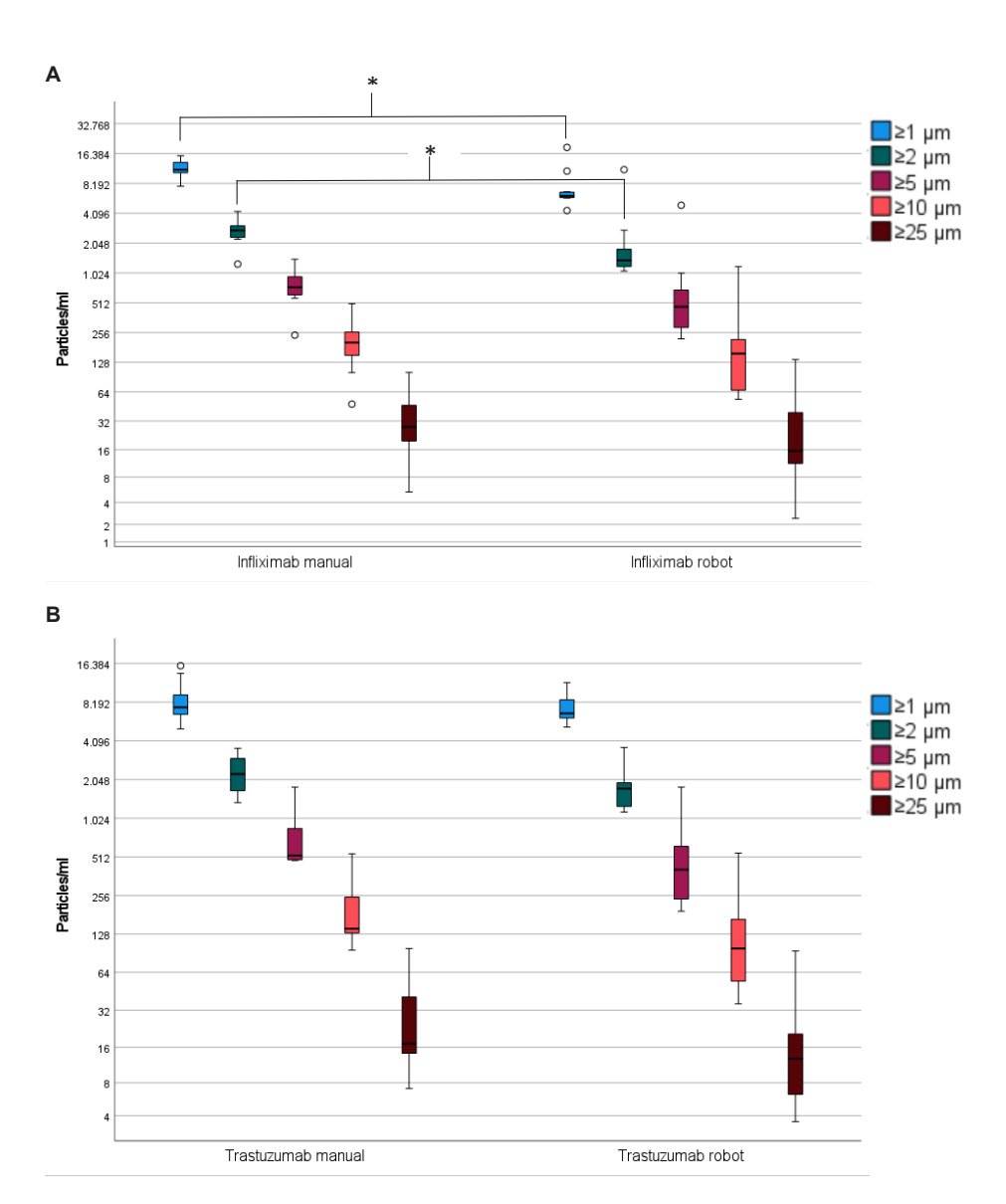


Fig. 4. Micro-Flow Imaging results (concentration of particles) in infliximab A) and trastuzumab B) infusion bags compounded with manual and robotic compounding. The boxplots show the median, interquartile range and the 5%/95% range with T-bars. Outliers are represented with open dots. The nonparametric Mann-Whitney U test was used for statistical analysis (*p < 0.05).

The number of particles measured with NTA was below the limit for quantitative analysis. Quantitative analysis would be possible if the concentration was within the detection limit of 10^7 particles/mL and 10^9 particles/mL, and if ≥ 200 tracks were found. The presence of fewer than 200 tracks in the software analysis indicated very poor statistics and therefore low confidence in the resulting particle distribution. None of the samples met these criteria. Only two samples had a concentration within the detection limit $(1.06*10^8$ and $2.71*10^8$ particles/mL); however, within these samples, either the number of tracks was below 200 or vibration was detected, making the data less reliable.

The DLS analysis of infliximab and trastuzumab infusion bags showed there were no statistical differences in monomer size (Z-average in nm) between samples from robotic compounding and conventional manual compounding (fig. 2). The median Z-average for manual- and robotic compounded infliximab was 12.5 nm (interquartile range; IQR: 12.4-12.7) and 12.4 nm (IQR 12.3-12.6), respectively. The monomer size of trastuzumab was ~1.5 nm smaller than infliximab, with a Z-average of 11.1 nm (IQR 11.0-11.1) and 11.0 (IQR 11.0-11.1) for manual- and robotic compounded trastuzumab, respectively.

The median PdI for infliximab was statistically lower for robotic compounding (0.12, IQR 0.11-0.15) compared with conventional manual compounding (0.16, IQR 0.14-0.18). The median PdI for trastuzumab was smaller than for infliximab and was not statistically different between both compounding methods, at 0.08 (IQR 0.07-0.11) and 0.08 (IQR 0.07-0.09) for manual- and robotic compounding, respectively (fig. 2).

LO results for infliximab showed the concentration of particles $\geq 1~\mu m$ was statistically significantly lower for robotic compounding than for conventional manual compounding, while the concentrations of particles $\geq 2~\mu m$, $\geq 5~\mu m$, $\geq 10~\mu m$, and $\geq 25~\mu m$ were not statistically different between both compounding methods. For trastuzumab, the concentrations of all different particle sizes ($\geq 1~\mu m$, $\geq 2~\mu m$, $\geq 5~\mu m$, $\geq 10~\mu m$, and $\geq 25~\mu m$) were not statistically different between manual and robotic compounding (fig. 3).

With MFI, the concentrations of particles $\geq 1~\mu m$ and $\geq 2~\mu m$ in the infliximab bags were statistically lower for robotic compounding than for manual compounding, while the concentrations of particles $\geq 5~\mu m$, $\geq 10~\mu m$, and $\geq 25~\mu m$ were not statistically different between both compounding methods. For trastuzumab, the concentrations of all particle sizes ($\geq 1~\mu m$, $\geq 2~\mu m$, $\geq 5~\mu m$, $\geq 10~\mu m$, and $\geq 25~\mu m$) were not statistically different between robotic compounding and manual compounding (fig. 4). Filtering out silicone oil (aspect ratio ≥ 0.85 = silicone oil) or air (circularity >0.9) did not affect the overall trends, and therefore we only report the total number of particles.

Images of the measured particles were also captured with MFI. Based on morphological parameters, particles can typically be associated with different types, such as protein particles, silicone oil microdroplets, air bubbles, and rubber fragments. Almost all particles appeared to be similar to those generally categorized as protein aggregates (fig. 5).

	Inflix	imab	Trastu	zumab
Particle size (μm)	Manual	Robotic	Manual	Robotic
5-10		A	1	
10-15	No.		-	
15-25	٥	L	6	1
25-40	8			Many.
40-50		No.	evel.	W
50-70	P			Con
70-100	with the same of t	and I	A CO	de

Fig. 5. Visualisation of representative particle types, captured with MFI, present in the manually and robotically compounded infusion bags containing infliximab or trastuzumab.

All infusion bags, including all negative controls, contained visible particles. Most visible particles in the trastuzumab, infliximab, and negative control bags had a white color and were shaped like thin fibers. The texture looked bumpy and the particles looked easily bendable (supplemental information, fig. 1).

Positive control samples, exposed to mechanical stress and shake stress (15 AD cycles and 16 hours of shaking), showed a strong increase in mAb aggregates (supplemental information, table 2). MFI and LO showed an increase in particle concentration, and DLS showed an increase in particle size and PdI.

DISCUSSION

The goal of this research was to compare the quality of compounded mAb products after manual compounding versus robotic compounding with respect to antibody stability and formation of (sub)visible aggregates. The quality of infliximab and trastuzumab was analyzed using six analytical techniques: high-performance size exclusion chromatography (HP-SEC), nanoparticle tracking analysis (NTA), dynamic light scattering (DLS), light obscuration (LO), micro-flow imaging (MFI), and visual inspection.

This study shows that robotic compounding of mAbs can provide similar pharmaceutical quality to manual compounding. The compounding method had a minor impact on the number of particulate aggregates. HP-SEC results (\approx 99.5% monomer content for all groups) indicate that there were no differences in the amount of dimers or other oligomers between robotic and manual compounded samples. LO and MFI results showed that the infusion bags with mAbs differ slightly in terms of particles from the negative controls performed with 0.9% sodium chloride, while positive controls show far higher particle numbers (supplemental information, table 2). Furthermore, DLS confirmed monodisperse samples, and the NTA results confirm a low level of protein aggregation after both manual and robotic compounding because all results were below the limit for quantitative analysis. These results could be clinically relevant because Kijanka et al., among others, have shown that submicron-size aggregates (100 nm - 1 μ m), which are measured with NTA, are more immunogenic than soluble oligomers (<100 nm) or micron-size (>1 μ m - 100 μ m) particles.

Although DLS showed PdI values <0.2, which implies relatively monodisperse samples, for both infliximab and trastuzumab, its standard deviation for manual compounding was larger than for robotic compounding, indicating more consistent and reproducible results with robotic compounding. One infusion bag of infliximab compounded

manually by a nurse showed a much higher Z-average. This could be due to less careful handling of the antibody during compounding. However, no deviating results were found with the other analytical techniques for the same infusion bag, which did not reinforce this interpretation. The hydrodynamic diameter determined by DLS was 12.5 nm for infliximab and 11.0 nm for trastuzumab. For infliximab, this is in line with earlier research, which reported a Z-average of 12.58 nm on day 0.²¹ For trastuzumab this was a bit higher than earlier research, which reported a Z-average of 10.3 nm with unstressed trastuzumab (originator, Herceptin®).²² The difference could be due to the presence of soluble aggregates after compounding of trastuzumab in infusion bags, which increased the Z-average.

LO and MFI results showed no relevant statistically significant differences for particles in trastuzumab and infliximab infusion bags. Less particles were found in the size range from 1-5 µm in infliximab bags after robotic compounding (fig. 3-4), however it is known that the variability in particle concentrations detected by LO and MFI is higher in this size range.²³ Micro-flow imaging (MFI) has been shown to provide higher sensitivity in detecting and imaging transparent particles and a unique capability to differentiate particle sub-populations with different morphologies using image filtering with a minimum size of 4 μm. ²³ LO underestimates smaller transparent particles <10 μm and is restricted in differentiating these particles based on morphology. European Pharmacopoeia criteria regarding the maximum number of sub-visible particles only exist for registered pharmaceutical intravenous preparations like the sodium chloride bags we used for compounding. Preparations comply with the LO test, if the average number of particles ≥10 µm present in the units tested does not exceed 25/mL, and the average number of particles ≥25 μm does not exceed 3/mL.²⁴ Half of our bags with mAbs met the European Pharmacopoeia criteria with LO. The numbers of particles were logically higher in the bags with mAbs compared to the negative controls for which the European Pharmacopoeia criteria apply.

Visual inspection showed particles in all investigated infusion bags, including all negative controls, which were unexpected because in daily practice we never see big particles in infusion bags before or after compounding. Also, European Pharmacopoeia criteria require registered intravenous preparations to be practically free of visible particles. ²⁵ In the absence of chemical analysis, it is difficult to comment on the exact nature of these particles. However, since all negative controls also contained visible particles, we expect that these particles were not proteinaceous. They could be generated due to the way we extracted the samples in this particular study.

This study investigated compounding of authorized drugs in routine hospital settings. Six complementary analytical methods were combined to assess different critical quality attributes (COAs): particle concentration, particle size, and percentage of protein aggregation. 26-28 This comprehensive analysis is necessary because investigating only one COA is misleading and potentially dangerous.²⁹ Both LO and MFI measure particles in the micron size range, while DLS and NTA support each other for particles in the submicron range. HP-SEC can strengthen these findings by quantifying the amount of monomer, dimer, and oligomers, and visual inspection adds information about particles ≥100 µm. The results of the six analytical methods together are in line with the results of Peters et al. Both studies indicate that robotic and manual compounding provide comparable antibody stability and formation of aggregates, with the robot generally giving more reproducible results. Other areas of interest with regards to robotic compounding such as time consummation, costs, microbiological quality and environmental contamination have been studied previously. 9,10,12,30 This study shows robotic compounding of mAbs provides products of similar pharmaceutical quality when compared to manual compounding.15

A limitation of the present study is that it was performed at a single center with one single robotic system and using only two products. Hence, our results cannot be extrapolated to other pharmacies with different compounding robots and other mAb products. For future research, it would be interesting to study the association between the number of particles in infusion bags and clinical outcomes, such as adverse effects and/or effective treatment results. This could be achieved by analyzing manual and robotic compounded infusion bags immediately before patient administration.

CONCLUSION

The APOTECAchemo robot is suitable for compounding mAbs since the quality is at least comparable with conventional manual compounding.

REFERENCES

- 1. Batson S, Mitchell SA, Lau D, et al. Automated compounding technology and workflow solutions for the preparation of chemotherapy: a systematic review. *European journal of hospital pharmacy*: science and practice 2020; **27**(6): 330-6.
- Gilbert RE, Kozak MC, Dobish RB, et al. Intravenous Chemotherapy Compounding Errors in a Follow-Up Pan-Canadian Observational Study. *J Oncol Pract* 2018; 14(5): e295-e303.
- Shin S, Koo J, Kim SW, Kim S, Hong SY, Lee E. Evaluation of Robotic Systems on Cytotoxic Drug Preparation: A Systematic Review and Meta-Analysis. Medicina 2023; 59(3): 431.
- 4. Yaniv AW, Orsborn A, Bonkowski JJ, et al. Robotic i.v. medication compounding: Recommendations from the international community of APOTECAchemo users. *Am J Health Syst Pharm* 2017; **74**(1): e40-e6.
- 5. Iwamoto T, Morikawa T, Hioki M, Sudo H, Paolucci D, Okuda M. Performance evaluation of the compounding robot, APOTECAchemo, for injectable anticancer drugs in a Japanese hospital. *J Pharm Health Care Sci* 2017; **3**: 12.
- 6. Zamani M, Chan K, Wilcox J. Pharmacy Technicians' Perceptions of Risk Reduction Strategies Implemented in Response to the Repetitive Strain Injury Associated with Sterile Compounding. *International journal of pharmaceutical compounding* 2021; **25**(3): 182-6.
- Bos JD, Meinardi MM. The 500 Dalton rule for the skin penetration of chemical compounds and drugs. Exp Dermatol 2000; 9(3): 165-9.
- 8. Geersing TH, Pourahmad DM, Lodewijk F, Franssen EJF, Knibbe CAJ, Crul M. Analysis of production time and capacity for manual and robotic compounding scenarios for parenteral hazardous drugs. *European Journal of Hospital Pharmacy* 2024; **31**(4): 352-7.
- 9. Baan SD, Geersing TH, Crul M, Franssen EJF, Klous MG. An economic evaluation of vial sharing of expensive drugs in automated compounding. *International journal of clinical pharmacy* 2022; **44**(3): 673-9.
- Geersing TH, Franssen EJF, Pilesi F, Crul M. Microbiological performance of a robotic system for aseptic compounding of cytostatic drugs. Eur J Pharm Sci 2019; 130: 181-5.
- 11. Geersing TH, Klous MG, Franssen EJF, van den Heuvel JJG, Crul M. Robotic compounding versus manual compounding of chemotherapy: Comparing dosing accuracy and precision. *Eur J Pharm Sci* 2020; **155**: 105536.
- 12. Werumeus Buning A, Geersing TH, Crul M. The assessment of environmental and external cross-contamination in preparing ready-to-administer cytotoxic drugs: a comparison between a robotic system and conventional manual production. *Int J Pharm Pract* 2020; **28**(1): 66-74.
- 13. Jiskoot W, Nejadnik MR, Sediq AS. Potential Issues With the Handling of Biologicals in a Hospital. Journal of pharmaceutical sciences 2017; **106**(6): 1688-9.
- Nejadnik MR, Randolph TW, Volkin DB, et al. Postproduction Handling and Administration of Protein Pharmaceuticals and Potential Instability Issues. *Journal of pharmaceutical sciences* 2018; 107(8): 2013-9.
- 15. Peters BJ, Capelle MA, Arvinte T, van de Garde EM. Validation of an automated method for compounding monoclonal antibody patient doses: case studies of Avastin (bevacizumab), Remicade (infliximab) and Herceptin (trastuzumab). *mAbs* 2013; **5**(1): 162-70.
- Doevendans E, Schellekens H. Immunogenicity of Innovative and Biosimilar Monoclonal Antibodies. Antibodies (Basel) 2019; 8(1).

- 17. Filipe V, Jiskoot W, Basmeleh AH, Halim A, Schellekens H, Brinks V. Immunogenicity of different stressed IgG monoclonal antibody formulations in immune tolerant transgenic mice. *mAbs* 2012; **4**(6): 740-52.
- 18. Filipe V, Hawe A, Jiskoot W. Critical evaluation of Nanoparticle Tracking Analysis (NTA) by Nano-Sight for the measurement of nanoparticles and protein aggregates. *Pharmaceutical research* 2010; **27**(5): 796-810.
- 19. Vlieland ND, Nejadnik MR, Gardarsdottir H, et al. The Impact of Inadequate Temperature Storage Conditions on Aggregate and Particle Formation in Drugs Containing Tumor Necrosis Factor-Alpha Inhibitors. *Pharmaceutical research* 2018; **35**(2): 42.
- 20. Kijanka G, Bee JS, Korman SA, et al. Submicron Size Particles of a Murine Monoclonal Antibody Are More Immunogenic Than Soluble Oligomers or Micron Size Particles Upon Subcutaneous Administration in Mice. *Journal of pharmaceutical sciences* 2018; **107**(11): 2847-59.
- 21. Tokhadze N, Chennell P, Le Basle Y, Sautou V. Stability of infliximab solutions in different temperature and dilution conditions. *Journal of pharmaceutical and biomedical analysis* 2018; **150**: 386-95.
- 22. Ahmadi M, Bryson CJ, Cloake EA, et al. Small amounts of sub-visible aggregates enhance the immunogenic potential of monoclonal antibody therapeutics. *Pharmaceutical research* 2015; **32**(4): 1383-94.
- 23. Sharma DK, King D, Oma P, Merchant C. Micro-flow imaging: flow microscopy applied to subvisible particulate analysis in protein formulations. *The AAPS journal* 2010; **12**(3): 455-64.
- 24. Ph. Eur. 11th edition, monograph 2.9.19. particulate contamination: sub-visible particles.
- 25. Ph. Eur. 11th edition, monograph 2.9.20. particulate contamination: visible particles.
- 26. Leja N, Wagner D, Smith K, Hurren J. Transportation of a commercial premixed intravenous insulin product through a pneumatic tube system. *Am J Health Syst Pharm* 2021; **78**(18): 1720-3.
- 27. Bakri SJ, Snyder MR, Pulido JS, McCannel CA, Weiss WT, Singh RJ. Six-month stability of bevacizumab (Avastin) binding to vascular endothelial growth factor after withdrawal into a syringe and refrigeration or freezing. *Retina (Philadelphia, Pa)* 2006; **26**(5): 519-22.
- 28. Kongmalai T, Chuanchaiyakul N, Sripatumtong C, et al. The effect of temperature on the stability of PCSK-9 monoclonal antibody: an experimental study. *Lipids Health Dis* 2021; **20**(1): 21.
- 29. van den Berg R, Mastrobattista E, Jiskoot W. Claiming therapeutic protein stability in a clinical setting based on limited analytical data is misleading and dangerous. *Am J Health Syst Pharm* 2022; **79**(8): 622-3.
- 30. Geersing TH, Pourahmad DM, Lodewijk F, Franssen EJF, Knibbe CAJ, Crul M. Analysis of production time and capacity for manual and robotic compounding scenarios for parenteral hazardous drugs. European journal of hospital pharmacy: science and practice 2023.

SUPPLEMENTAL MATERIALS

Supplementary table 1. Results of the preliminary analysis of transport from Amsterdam to Leiden of four trastuzumab and infliximab infusion bags.

HP-SEC	Amount monomer (%)	Amount dimer (%)	Amount HMW (%)
Bag 1: trastuzumab 150mg, Leiden	99.7	0.3	0.0
Bag 2: trastuzumab 150mg, Amsterdam	99.6	0.4	0.0
Bag 3: infliximab 100mg, Leiden	99.4	0.6	0.0
Bag 4: infliximab 100mg, Amsterdam	99.4	0.6	0.0

NTA

The number of particles measured with NTA were below the limit for quantitative analysis.

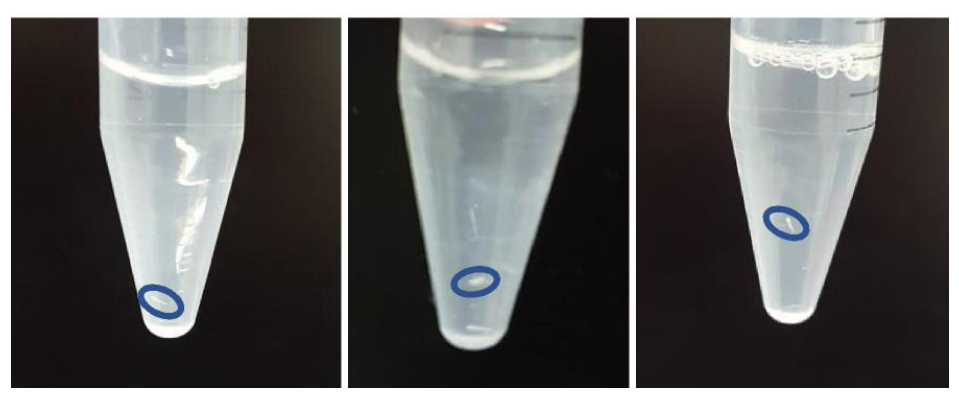
DLS	Z-ave (nm)	PdI	Z-ave (nm)	PdI	
Bag 1: trastuzumab 150mg, Leiden	11.11	0.13	11.09	0.15	
Bag 2: trastuzumab 150mg, Amsterdam	11.15	0.06	11.14	0.10	
Bag 3: infliximab 100mg, Leiden	13.21	0.24	13.01	0.22	
Bag 4: infliximab 100mg, Amsterdam	12.31	0.13	12.35	0.15	
LO	≥1 µm	≥2 µm	≥5 µm	≥10 µm	≥25 µm
Bag 1: trastuzumab 150mg, Leiden	1516	339	39	8	0
Bag 2: trastuzumab 150mg, Amsterdam	1256	398	94	18	1
Bag 3: infliximab 100mg, Leiden	3589	778	183	39	6
Bag 4: infliximab 100mg, Amsterdam	4743	1042	157	24	2
MFI	≥1 µm	≥2 µm	≥5 μm	≥10 µm	≥25 µm
Bag 1: trastuzumab 150mg, Leiden	3812	980	109	21	1
Bag 2: trastuzumab 150mg, Amsterdam	2790	703	118	36	11
Bag 3: infliximab 100mg, Leiden	18287	3689	911	238	50
Bag 4: infliximab 100mg, Amsterdam	19044	5124	796	106	8

VΙ

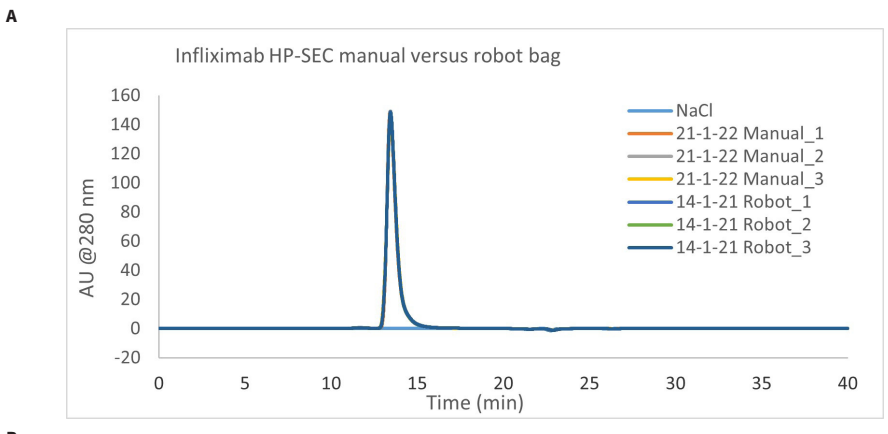
All four bags contained visible particles. Visible particles had a white color and were shaped like thin fibers.

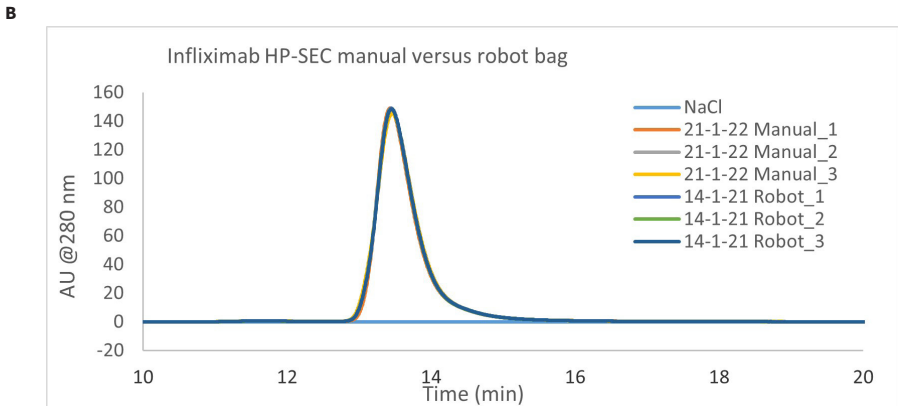
Supplementary table 2. Overview of the negative (sodium chloride 0.9%) and positive controls (aspirate/dispense cycles followed by shaking) analyzed with LO and MFI.

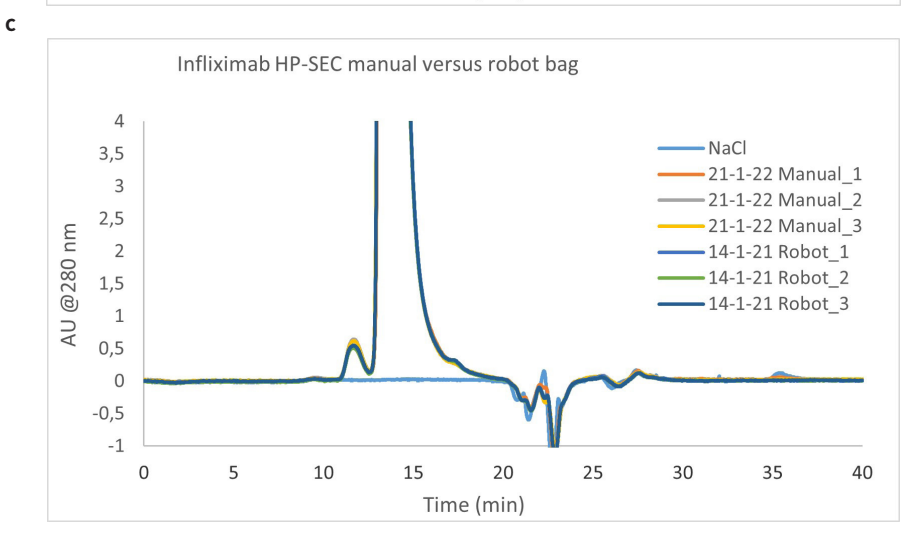
	≥1 µm	≥2 µm	≥5 µm	≥10 µm	≥25 µm
го					
Negative control, sodium chloride 0.9%	630	76	7	2	0
Positive control, trastuzumab	73421	9808	852	88	2
Positive control, infliximab	109933	40350	9954	1255	93
MFI					
Negative control, sodium chloride 0.9%	5779	984	137	56	2
Positive control, trastuzumab	300450	11111	5417	521	26
Positive control, infliximab	820980	161402	163262	44233	1782



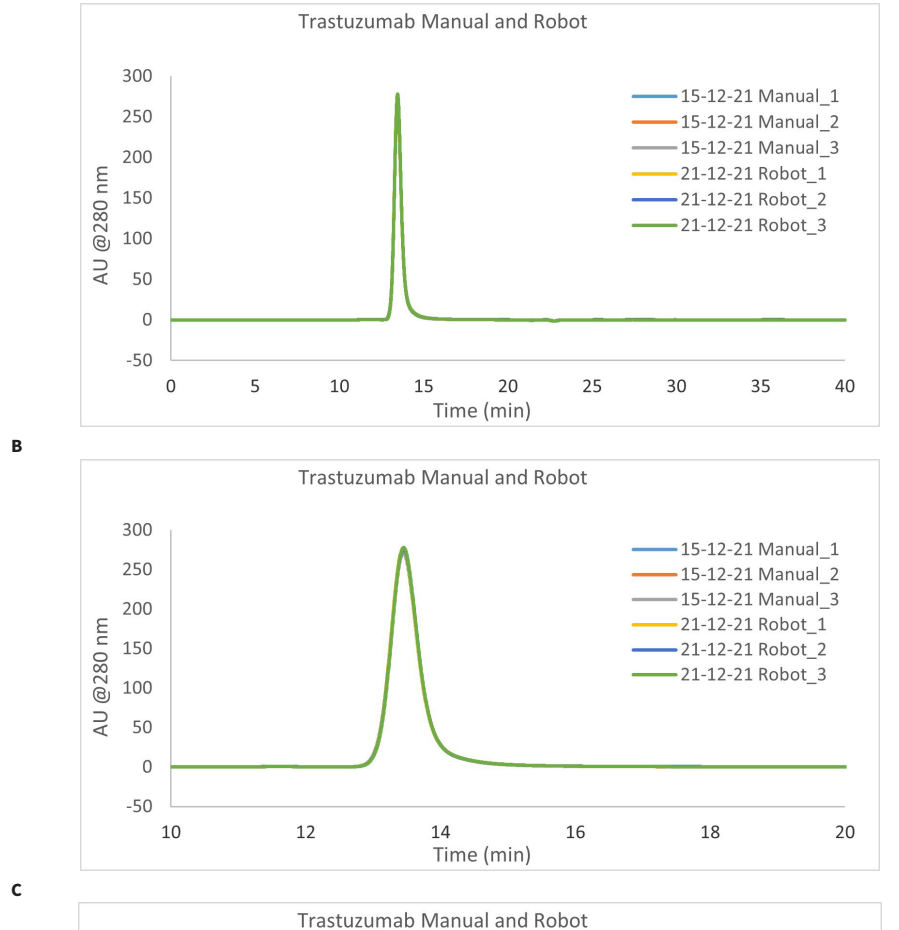
Supplementary fig. 1. Visualization of particles (in the blue ovals) present in the samples withdrawn from the negative controls (left picture), manual and robotic compounded infusion bags containing infliximab (middle picture) or trastuzumab (right picture) as captured by visual inspection.



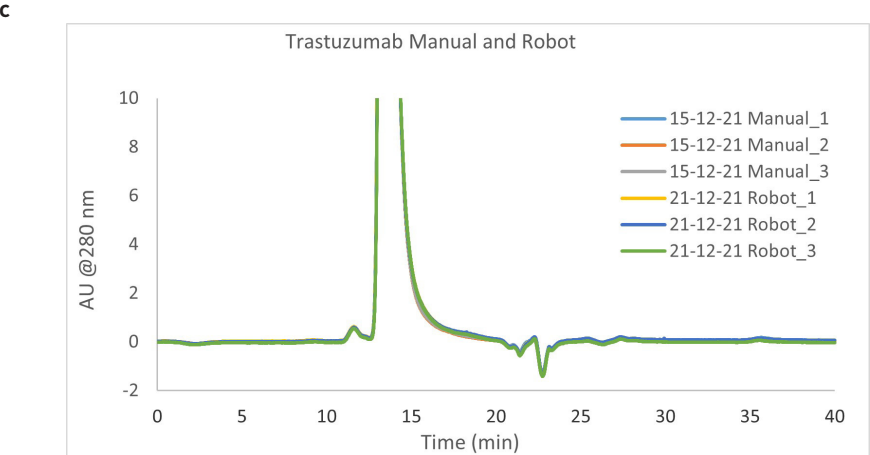




Supplementary fig. 2. Examples of HP-SEC chromatograms of a robotic and a manual compounded infliximab infusion bag. Three samples were taken out of every infusion bag. In fig. A, the analysis period from 0-40 minutes is shown, in B the period from 10-20 minutes and in C is zoomed in on the y-axis.



Α



Supplementary fig. 3. Examples of HP-SEC chromatograms of a robotic and a manual compounded trastuzumab infusion bag. Three samples were taken out of every infusion bag. In fig. A, the analysis period from 0-40 minutes is shown, in B the period from 10-20 minutes and in C is zoomed in on the y-axis.